PAPER • **OPEN ACCESS**

Size-dependent phase stability of silver nanoparticles

To cite this article: A M Murzakaev 2020 *IOP Conf. Ser.: Mater. Sci. Eng.* **1008** 012003

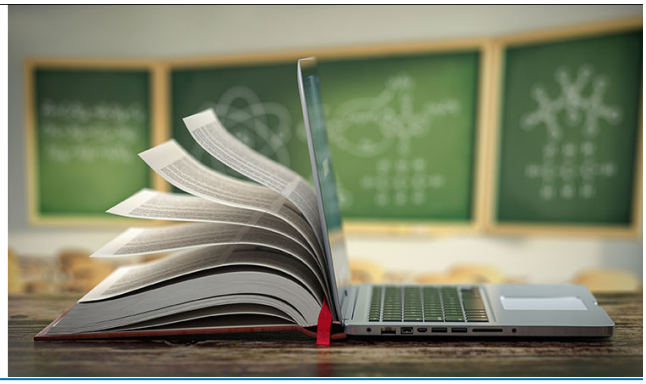

Size-dependent phase stability of silver nanoparticles

A M Murzakaev[1,2]

[1]Institute of Electrophysics UB of RAS, 620016, Yekaterinburg, 106 Amundsena St., Russia
[2]Ural Federal University, 620002, Yekaterinburg, 19 Mira St., Russia

E-mail: Amurzak@mail.ru , Aidar@iep.uran.ru

Abstract. A comparative analysis of the structure of silver nanoparticles obtained by chemical synthesis (citrate method) and electrical explosion of wires is carried out. The structure, phase composition, lattice parameters of silver nanoparticles with sizes from 2 to 50 nm were studied by electron diffraction and high-resolution transmission electron microscopy. All silver nanoparticles obtained by the chemical method have only a cubic structure. Silver nanoparticles obtained by the physical method have cubic and hexagonal structures. The existence of the hexagonal phase under normal conditions is explained by the quenching effect. The lattice parameters of the cubic phase of Ag NPs within the experimental determination error (± 0.01 nm), synthesized by the chemical method and by the method electrical explosion of wires do not differ from each other.

1. Introduction

Silver (Ag) nanocrystals have been widely used in several areas (catalysis, biological, antimicrobial, information storage, surface-enhanced Raman spectroscopy, interconnects in ultra large-scale integration circuits etc). It is well known that the physical properties of nanoparticles strongly depend on their microstructure. The crystal structure is a critical parameter for the determination of materials properties of the nanocrystals. Silver in its bulk form possesses a cubic crystal structure (Ag-FCC). The authors of [1] obtained a proof of the presence of a hexagonal phase (Ag-4H) in nuggets of silver. Later it was found that the Ag-4H is a stable phase when the particle size remains smaller than a critical size $d_c < 40$ nm. The stability of the hexagonal polymorph at room temperature and the normal atmospheric pressure has been often discussed in literature as a grain size effect. There are conflicting reports in the literature regarding the phase structure of Ag particles with sizes below 40 nm [2-7]. It is significant that many authors have generally confirmed these results, but the critical size appears to depend strongly on the physical and chemical synthesis techniques.

Changing the size will change the stability range of ordinary bulk materials. This phenomenon has been found in many oxide materials such as ZnO, ZrO_2, $A1_2O_3$, TiO_2, Fe_2O_3. Various explanations have been proposed for the observed stabilization of the high temperature phase in nanocrystalline oxide particles at room temperature, and controversies still exist in the elucidation of the mechanism of the phase stability. For example, Garvie [8] proposed that the lower surface energy of tetragonal (t) ZrO_2 was the cause for this phase to be present in nanocrystalline form at or below room temperature. He predicted that particles below about 10 nm in diameter are stabilized in the tetragonal form, and those that are above this critical particle size are subject to the monoclinic (m) transformation. Later, in [9] Murase and Kato suggested that water vapor increased the rate of crystallite growth and

decreased surface energy having thus significant effect on the t-m transformation. Domain boundaries were also suggested to inhibit the t-m transformation thus leading to tetragonal phase stability [10]. In [11] Srinivasan et al. argued against the concept proposed by Garvie (stabilization due to lower surface energy of the t phase) as they found monoclinic particles with much smaller diameters. They suggested that anionic oxygen vacancies present on the surface control the t-m phase transformation on cooling, and that oxygen adsorption triggers this phase transformation. All the articles cited here, except the one by Garvie [8], have in common that the zirconia nanoparticles were produced by various chemical methods (precipitation and calcination). Chemical factors such as adsorbed atoms and purity of raw materials play an important role in the stability of nanocrystalline zirconia and they may completely alter the original surface energy state. Therefore, none of the above explanations have a general validity for pure nanocrystalline zirconia. One of the most recent explanations is based on an increased effective internal pressure due to the surface curvature and the small particle radius (the Gibbs-Thomson effect): $\Delta p = 2\gamma/r$, where Δp is the difference between the external and the internal pressure, γ is the surface energy, and r is the particle radius [12]. This explanation has been since then quite often used for several nanocrystalline ceramic systems as the stabilization of high-temperature or high-pressure polymorph in nanoparticles appeared to be a more general phenomenon. This size-dependent phenomenon is independent of the fabrication method. One of the main quantitative characteristics of nanoparticles is the Gibbs free surface energy. It differs significantly from the energy for macro objects. It has to be mentioned that other mechanisms were also proposed, e.g. a nanothermodynamic model was also established to reveal the origin of the size effect on the polymorphism (face centered cubic and 4H structures) behavior of Ag nanocrystals with the contributions of surface energy and surface stress to the total Gibbs free energy [7]. It shows that the lower surface energy and surface stress coupled with a higher volume of the Gibbs free energy predominates the thermal stability of 4H-structured Ag in a nanometer scale. A thermodynamic explanation has also been developed to calculate the r_c of Ag nanoparticles at different temperatures [7]. The $d_c(T)$ function of Ag nanocrystals was also obtained with respect to the thermodynamic consideration of $G^{FCC}(r,T) = G^{4H}(r,T)$. Furthermore, several thermodynamic parameters of the Ag-4H are also determined with the developed model.

In this paper, results of detailed studies on the morphology and crystal structure of Ag nanoparticles produced by chemical method and electrical explosion of wire are presented.

2. Experimental

Silver nanoparticles were synthesized by the physical method using electrical explosion of wire (EEW) as described in detail in [13] and the chemical method using a chemical reduction of $AgNO_3$ with N_2H_5OH in the presence of Na-cit as described in detail in [14]. The minimum size of silver nanoparticles was specially obtained by the chemical method. According to [15], the initial stage of reduction yields clusters Ag_2^+, Ag_4^+, Ag_9^+, etc. The nascent Ag_x clusters reacted with citrate, which was followed by their aggregation into coarser particles. Upon reaching the critical size (50 - 100 atoms or 1 - 1.5 nm), the clusters virtually cease to grow by the condensation mechanism. Further clusters growth is highly dependent on the citrate concentration. The growth of NPs at intermediate citrate concentrations, namely, $(1\text{-}5)\bullet10^{-4}$ mol litre^{-1}, occurred as a result of reduction of silver ions on the cluster surface. Hence, after the cluster nucleation, its further growth proceeded gradually. Silver NPs formed by this mechanism were unsusceptible to aggregation, spherical and had narrow size distribution. At low citrate concentrations, its stabilizing action was insufficient to prevent the aggregation of clusters, which led to NPs of larger diameters. At higher citrate concentrations, the solution ionic strength reached large magnitudes sufficient for the destabilization of the citrate layer, which also resulted in coagulation. Yellow sol was obtained by boiling solution at T = 100 °C.

With the use of x-ray phase analysis (D8 DISCOVER diffractometer, Germany), the phase composition, spacing parameters, and the size of the coherent scattering regions (CSR) were determined. The diffractograms were handled with the use of the TOPAS 3 software. The error of determining the content of phases was about 2 wt%. The particle morphology was studied by

transmission electron microscopy (TEM) and scanning electron microscopy (SEM) by microscopes JEM-2100 and LEO-982. Selected-area electron diffraction (SAED) and high-resolution transmission electron microscopy HRTEM (JEM 2100) have been used to determine the morphological and phase features of silver nanoparticles. The calibration of the magnification of the HRTEM and the determination of the device constant for the electron diffraction measurements were performed using a gold foil. This choice is due to the fact that the structure of gold is well known, it rarely has defects, and its interlayer distances are 0.23 nm and 0.20 nm (which corresponded to planes (111) and (200) well resolved by the device); in addition, the electron diffraction pattern of gold can easily be interpreted. The processing and analysis of the images were performed using the 3.9.3 version of the Gatan Digital Micrograph program, which allowed us to calibrate images, to apply masks and filters, to perform fast Fourier-transformations (FFT) both of the entire photograph and of the selected regions, to perform measurements, and to save data in various formats. The interplanar distances of the phases of the samples were taken from the Powder Diffraction File.

3. Results and discussion

3.1. EEW nanopowders

The electric explosion of a wire represents a rapid change in the physical state of a metal as a result of intense heat generation when a high-density pulse current is transmitted. As a result of the passage of a current pulse, the metal overheats above the melting temperature, and the superheated metal is explosively dispersed. The pressure and temperature at the front of the emerging shock wave reach several hundred megapascals and approximately 10^4 K, respectively. As a result of condensation in a stream of rapidly expanding steam, particles of very small sizes are formed. By adjusting the conditions of the explosion, it is possible to obtain powders with particles of different sizes - from 5 to 300 nm (the weighted average particle radius is 70 nm or more). Results of the XDR analysis of the silver nanoparticles showed that more than 97% mass. had a cubic structure ($a = (0.4082 \pm 0.0007)$ nm) with CSR 21 nm, less than 3 % mass. had a hexagonal structure.

3.2. Chemical nanopowders

The EDX analysis was performed on three sample sites. The analysis showed the absence of possible impurities from elements (N, O) in the samples. From these results, it can be concluded that the silver nanoparticles are pure. The results of the XDR analysis of the silver nanoparticles obtained via the chemical method showed only a cubic structure ($a = (0.4085 \pm 0.0007)$ nm) with a CSR of 10 nm. Figure 1a shows TEM images of the synthesized silver nanoparticles. It can be observed that the silver nanoparticles have a spherical shape. Both individual nanoparticles and their agglomerates are present in the figure. Figure 1b shows the distribution of nanoparticles by size in yellow sols. The sol contains particles of different sizes - from 2 to 26 nm (the weighted average particle radius is 7 nm). The structure and phase composition of Ag nanoparticles were determined by the SAED method. The inset in figure 1a shows a SAED pattern of the prepared samples. The SAED pattern of the sample has a point-ring shape, which is indicative of the polycrystalline structure of the samples. All nanoparticles are crystalline, no amorphous nanoparticles were detected. The analysis of SAED patterns has confirmed the crystal structure of particles, which is indexed as a cubic (Fm3m) structure of Ag. An exact determination of the phase composition is possible from the analysis of HRTEM patterns of separate nanoparticles. Figure 1 c, d, e shows three particles of approximately the same size. Figure 1 c shows NPs obtained by the EEW method. The interplanar spacings were obtained from the FFT and they correspond to Ag-4H. In figure 1d,e NPs obtained by the chemical method are shown. The interplanar spacings are obtained from the FFT and correspond to Ag-FCC. After FFT of the whole figure 1e, masking on the FFT, and the reconstructed image by inverting the filtered image is shown in figure 1f. This picture clearly shows Ag clusters ranging in size from 1 to 1.5 nm and NPs up to 5 nm with a cubic structure. The processing of HRTEM images of Ag NPs obtained by the chemical method showed the presence of only the cubic phase. The minimum particle size obtained by the chemical

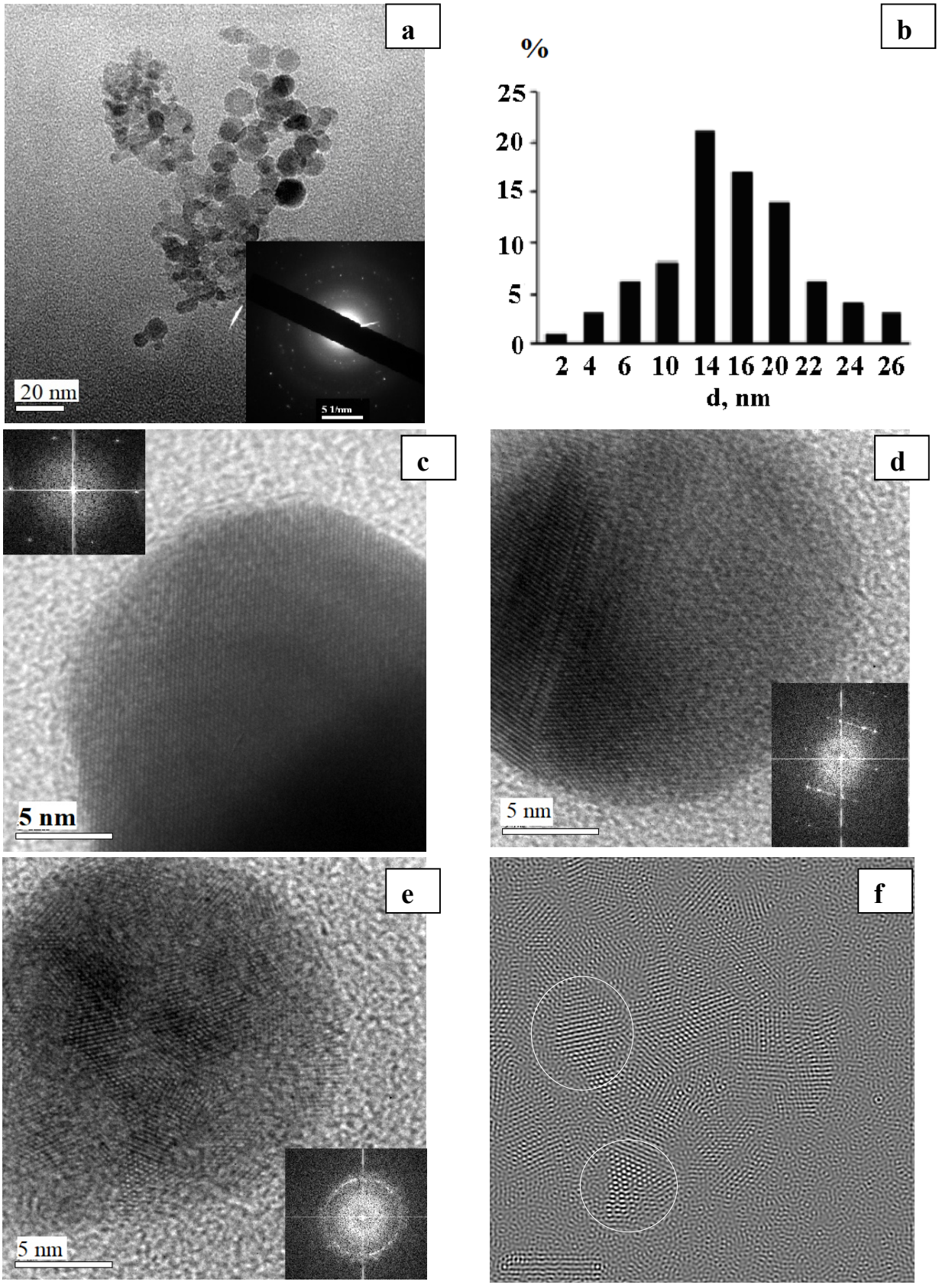
a
20 nm
5 1/nm
b
%
25
20
15
10
5
0
2 4 6 10 14 16 20 22 24 26
d, nm
c
5 nm
d
5 nm
e
5 nm
f

Figure 1.

method is an order of magnitude smaller than the particle size obtained by the EEW method.

Despite this, there are no particles with a hexagonal phase among the particles obtained by the chemical method. The presence of Ag-4H in NPs obtained by the EEW method cannot be explained by the Gibbs-Thomson effect. On the other hand, as shown in [7], the $r_c(T)$ function decreases with increasing T and leads to a higher thermal stability of Ag-4H than Ag-FCC for small sizes of Ag nanocrystals at lower temperatures and vice versa. Thus, this model does not agree with the obtained experimental data.

Next comes the process of formation of the Ag-4H structure. Solidification of the NPs after EEW comes from undercooling of liquid droples. The cooling process is extremely short. The crystalline structure firstly formed in the nanoparticle corresponds to the phase diagram of the material and conforms to the temperature at the point in time of nucleus appearance and the increased surface tension of the nanoparticle. The delay in the transformation into a stable lattice take place due to the extremely short cooling process as well as the perfect structure of nanoparticles (Fig. 1c), in which defects, acting as possible nucleation centres, are rare. After cooling at room temperature, lattice transformation is not possible, since the minimum value of energy required for homogeneous nucleation is an insurmountable barrier. As a result, the nanoparticles produced with EEW are "frozen" in the metastable lattice.

Within the experimental determination error (± 0.01 nm), the lattice periods of Ag NPs synthesized by the chemical method and by the method of wire electric explosion do not differ from each other. It has been established that the unit cell parameter of clusters ranging in size from 1 to 1.5 nm and Ag NPs is not a size-dependent quantity and, within the measurement error, takes on a value characteristic of the bulk state. The results obtained contradict the model concepts put forward in [10].

Conclusion

Studies using a transmission electron microscope have convincingly shown that Ag NPs obtained by the chemical method have only a cubic structure. Ag NPs obtained by the EEW method contain both hexagonal and cubic phases. Based on the analysis of the conditions for obtaining Ag NPs, the mechanism of stabilization of the hexagonal phase under normal conditions is explained by the quenching effect. The lattice periods of the cubic phase of Ag NPs within the experimental determination error (± 0.01 nm), synthesized by the chemical method and by the electrical explosion of wire do not differ from each other.

References

[1] Novgorodova M I, Gorshkov A I and Mokhov A V 1981 *Int. Geol. Rev.* **23(4)** 485
[2] Bublik A I 1954 *Dokl. Academy of Sciences the USSR* **95** 521
[3] Taneja P, Banerjee R, Ayyub P, Chandra R and Dey G K 2001 *Phys. Rev*. B **64** 033405
[4] Liu X H, Luo J and Zhu J 2006 *Nano Lett*. **6** 408
[5] Liang C H, Terabe K, Hasegawa T and Aono M 2006 *Japan. J. Appl. Phys.* **45(7)** 6046-48
[6] Singh A and Ghosh A 2008 *J. Phys. Chem*. **112(10)** 3460
[7] Yang C C and Li S 2008 *J. Phys. Chem.* C **112(42)** 16400
[8] Garvie R C 1965 *J. Phys. Chem*. **69** 1238
[9] Muraze Y and Kato E 1983 *J. Am. Ceram. Soc.* **66** 196
[10] Mitsuhashi T, Ichihata M and Tatsuke U 1974 *J. Am. Ceram. Soc.* **57** 97
[11] Srinivasan R, Rice L, Davis B H 1990 *J. Am. Ceram. Soc.* **73(11)** 3528
[12] Skandan G, Foster C M, Frase H, Ali M N, Parker J C and Hahn H 1992 *Nanostr. Mater*. 1 313
[13] Murzakaev A M 2017 *Phys. Met. Metallogr.* **118(5)** 459
[14] Brainina Kh Z, Galperin L G, Kiryuhina T Yu, Galperin A L, Stozhko N Yu, Murzakaev A M and Timoshenkova O R 2012 *J. Sol. St. Electrochem*. **16** 2365
[15] Krutyakov Yu A, Kudrinskiy A A, Olenin A Yu and Lisichkin G V 2008 *Russ. Chem. Rev.* **77(3)** 233
[16] Qi W H and Wang M P 2005 *J. Nanopart. Res*. **7** 51